UCRL-TR-203199

LAWRENCE
LIVERMORE
NATIONAL
LABORATORY

Fermion Monte Carlo Calculations on Liquid-3He

L. Colletti, F. Pederiva, M. H. Kalos

March 26, 2004

Disclaimer

This document was prepared as an account of work sponsored by an agency of the United States Government. Neither the United States Government nor the University of California nor any of their employees, makes any warranty, express or implied, or assumes any legal liability or responsibility for the accuracy, completeness, or usefulness of any information, apparatus, product, or process disclosed, or represents that its use would not infringe privately owned rights. Reference herein to any specific commercial product, process, or service by trade name, trademark, manufacturer, or otherwise, does not necessarily constitute or imply its endorsement, recommendation, or favoring by the United States Government or the University of California. The views and opinions of authors expressed herein do not necessarily state or reflect those of the United States Government or the University of California, and shall not be used for advertising or product endorsement purposes.

This work was performed under the auspices of the U.S. Department of Energy by University of California, Lawrence Livermore National Laboratory under Contract W-7405-Eng-48.

Fermion Monte Carlo calculations on liquid-^{3}He

Leonardo Colletti*
INFM and Dipartimento di Fisica, Università di Trento, I-38050 Povo(TN), Italy and Department of Computer Science, Free University of Bolzano/Bozen, 39100 Bolzano, Italy

Francesco Pederiva†
INFM and Dipartimento di Fisica, Università di Trento, I-38050 Povo(TN), Italy

Malvin H. Kalos‡
Lawrence Livermore National Laboratory, University of California, Livermore, California 94551
(Dated: March 24, 2004)

Methods and results for calculations of the ground state energy of the bulk system of ^{3}He atoms are discussed. Results are encouraging: we believe that they demonstrate that our methods offer a solution of the "fermion sign problem" and the possibility of direct computation of many-fermion systems with no uncontrolled approximations. Nevertheless, the method is still rather inefficient compared with variational or fixed-node approximate methods. There appears to be a significant populations size effect. The situation is improved by the inclusion of "Second Stage Importance Sampling" and of "Acceptance/Rejection" adapted to our needs.

I. INTRODUCTION

Powerful Monte Carlo methods[1,2] can provide estimates of ground state properties of bosonic many-body systems that are not subject to uncontrolled approximations. This means that results are exact within statistical and systematic errors that can be reduced by extending the stochastic sampling, i.e. the length of the computer run, and, for example, by increasing the size of the system.

But the mapping of the many-body quantum wavefunction to a probability distribution function faces severe challenges when considering the global antisymmetry that a fermionic wavefunction must satisfy. This is the essential source of the "fermion sign problem"[3,4].

Why is the fermion problem difficult within the framework of Diffusion or Green's Function Monte Carlo? There are several somewhat distinct ways of describing the challenge; understanding them is the key to overcoming them.

We are required to find solutions to the Schrödinger equation that satisfy the Pauli principle– i.e., that the solution be antisymmetric. When the potential does not depend upon spins, that means that the solution changes sign on the interchange of the coordinates of like-spin particles. In turn that poses two difficulties: the first is that the solution is not everywhere positive, a situation that is not natural for diffusion or for Monte Carlo. At a formal level, we may answer this by introducing random walkers that carry signs, so that, at least in principle, a solution that is sometimes negative can be encompassed. As we shall see, that is not the end of the story. The second and deeper concern is that the Pauli principle is a global constraint that connects the solution at points far apart in configuration space. Diffusion Monte Carlo is local– the stochastic dynamics depends entirely upon the potential and the trial function evaluated at the position of a walker. Imposing a global constraint without introducing approximations is a challenge. One may regard the usual "fixed-node constraint" as just such an approximation.

If one simply carries out Diffusion Monte Carlo and attempts to extract (by projection) information about the antisymmetric solution, one encounters an exponential decay of signal relative to noise in the Monte Carlo results. This is a consequence of the asymptotic dominance of the symmetric ground state in the distribution of the walker positions. To counter this effect, it is necessary to cancel positive walkers against negative walkers. But this can only be done exactly if they meet. As is well known, independent random walkers meet with probability zero in domains greater than two dimensions. For our computations, in which very large dimensional spaces are used, the walkers must be correlated in a way that permits them to meet with some finite probability.

Finally, one must take account of the following general result: given that we are using positive and negative walkers, and if the stochastic dynamics used are invariant under the interchange of the signs, the asymptotic density of walkers will be similarly invariant. In that case, the asymptotic value of any projection with an antisymmetric function will be zero. Therefore the dynamics for plus and minus walkers must be different in some way.

There is no unique algorithmic approach to these difficulties. The methods that we have adopted, and which are the basis of the results reported in this paper, are based on a population of pairs of positive and negative walkers which is generated using Diffusion Monte Carlo modified in the following ways:

(1) Different guiding functions are used for walkers of different signs; the two functions map into each other on application of an odd permutation applied to coordinates of like-spin particles.

(2) When walkers of different signs branch differently (as they must) new pairs are created by applying the

nearest pair permutation of like-spin particles to that walker with the greater weight.

(3) The "diffusion" steps of the walkers in a pair are correlated by reflecting one of the vectors of Gaussian random variables in the hyperplane that is the perpendicular bisector of the segment that connects the positions of the two walkers. This guarantees that the walkers can meet in any number of dimensions.

(4) Walkers in a pair that come close can be canceled in a way that guarantees that the future value of any projection with an antisymmetric function is exactly preserved. Thus there is no bias involved in this cancellation. Since the marginal walk for either member of a pair is otherwise just that of Diffusion Monte Carlo, the method has no bias associated with its fermion character. The usual time-step and population control biases remain, but they can be controlled in standard ways.

(5) We have been able to adapt the technique of "acceptance-rejection" to our method. We will compare computations with and without this feature.

(6) We have also experimented with a "Second-stage" importance sampling scheme, in which a function of the coordinates of both walkers of a pair is used to modify the distribution of the walkers.

More technical details on these points will be presented in Sec. II. Results obtained with and without items (5) and (6) are discussed and compared in Sec. III, along with experimental and fixed node Monte Carlo results.

II. THE METHOD

Let us consider a system of N atoms of which the coordinates of the ith particle are represented by a tridimensional vector $\mathbf{r_i}$. The atoms interact with one another via two- and three-body forces summarized by a potential $V(\mathbf{r_1}, ...\mathbf{r_N})$. Our primary interest is in the ground state energy E_0 of the system, for which we need to solve the many-body Schrödinger equation.

Simple Diffusion Monte Carlo follows the evolution in imaginary time; using atomic units, this equation translates into

$$\left[-\frac{1}{2}\nabla^2 + V(\mathbf{R}) - E_T\right]\psi(\mathbf{R},\tau) = -\frac{\partial\psi(\mathbf{R},\tau)}{\partial\tau} \qquad (1)$$

which is a diffusion equation (the kinetic part gives the diffusion operator) and absorption (associated with the potential energy), solved by iterating an appropriate Green's function $G(\mathbf{R},\mathbf{R}',\delta\tau)$ on the $3N$-dimensional vector $\mathbf{R}'(x_1, x_2, ..., x_{3N})$ that represents a whole configuration (a "walker") of the system,

$$\psi(\mathbf{R},\tau+\delta\tau) = \int G(\mathbf{R},\mathbf{R}',\delta\tau)\psi(\mathbf{R}',\tau)d\mathbf{R}' \qquad (2)$$

A formal solution of (1) can be written expanding $\psi(\mathbf{R},\tau)$ in a complete set of eigenfunctions as

$$\psi(\mathbf{R},\tau) = \sum_i N_i e^{-\tau(E_i-E_T)}\phi_i(\mathbf{R}) \qquad (3)$$

where E_i are the energy eigenvalues corresponding to the eigenfunctions $\phi_i(\mathbf{R})$ of the Hamiltonian, while E_T is a constant shift that has been subtracted for convenience from the total energy in order to mantain stable the population of walkers that undergoes the diffusion and selection process symbolized by (1). N_i are expansion coefficients that depend on the initial conditions.

At each step $\psi(\mathbf{R},\tau)$ is thus represented by an ensemble of discrete points $\{\mathbf{R}_m\}$ that are then advanced and reproduced or removed according to $G(\mathbf{R},\mathbf{R}',\delta\tau)$.

In the limit of sufficiently long imaginary-time τ, only the term with the lowest energy survives in (3)

$$\psi(\mathbf{R},\tau) = N_0 e^{-\tau(E_0-E_T)}\phi_0(\mathbf{R}) \qquad (4)$$

and, if $E_T = E_0$, the walkers $\{\mathbf{R}_m\}$ are sampled from a stationary probability density distribution that maps the symmetric, bosonic ground state $\phi_0(\mathbf{R})$.

A. Importance-sampled DMC

In order to improve the efficiency of this filtering of the solution, especially for systems with unbounded potential, one introduces a known trial wavefunction $\psi_T(\mathbf{R})$ with the aim of changing the sampling process in a known way[1] while preserving averages.

$\psi_T(\mathbf{R})$ biases the density of the walkers $\{\mathbf{R}_m\}$ to make them more likely to contribute to the future of the random walk. Hence one considers the new distribution function

$$f(\mathbf{R},\tau) = \psi_T(\mathbf{R})\psi(\mathbf{R},\tau) \qquad (5)$$

with $\psi(\mathbf{R},\tau)$ as in (3) and (1) becomes

$$-\frac{1}{2}\nabla^2 f + [E_L(\mathbf{R}) - E_T]f + \frac{1}{2}\nabla\cdot[f\nabla\ln|\psi_T(\mathbf{R})|^2] = -\frac{\partial f}{\partial\tau} \qquad (6)$$

where

$$E_L(\mathbf{R}) = \frac{\hat{H}\psi_T(\mathbf{R})}{\psi_T(\mathbf{R})} \qquad (7)$$

is the local energy, with $\hat{H}$ the Hamiltonian operator. Eq. (6) still represents a diffusion process for the $\{\mathbf{R}_m\}$, whose moves have a Gaussian distribution modified by a drift step that pushes the distribution towards the regions where $\psi_T(\mathbf{R})$ is larger.

After equilibration is reached, the distribution sampled is $\psi_T(\mathbf{R})\phi_\mathbf{0}(\mathbf{R})$ and the energy estimator is then calculated as an average of the local energies corresponding with the N_w sampled walkers $\{\mathbf{R}_m\}$

$$
\begin{aligned}
E_0 &= \frac{\int \hat{H}\psi_T(\mathbf{R})\phi_0(\mathbf{R})d\mathbf{R}}{\int \psi_T(\mathbf{R})\phi_0(\mathbf{R})d\mathbf{R}} \\
&= \frac{\int \hat{H}\psi_T(\mathbf{R})\frac{\phi_0(\mathbf{R})\psi_T(\mathbf{R})}{\psi_T(\mathbf{R})}d\mathbf{R}}{\int \psi_T(\mathbf{R})\phi_0(\mathbf{R})d\mathbf{R}} \\
&= \frac{\sum_m^{N_w} \frac{\hat{H}\psi_T(\mathbf{R_m})}{\psi_T(\mathbf{R_m})}}{N_w}. \qquad (8)
\end{aligned}
$$

For the fermionic case, a trial function needs of course to be antisymmetric under the exchange of two like-spin particles, thus it has to be orthogonal to the state $\phi_0(\mathbf{R})$ that is naturally filtered out by the DMC process. Hence the *fermion catastrophe*, i.e. decay of the overlap of the random-walk generated population $\phi_0(\mathbf{R})$ with $\psi_T(\mathbf{R})$, and the need of uncontrolled approximations like fixed node DMC that gives only an upper bound to the energy[5] or the transient released node method[6,7] that is essentially unstable.

B. Pair-based, Importance-sampled FMC

In our FMC algorithm this concept of trial function is split into two separate auxiliary functions: a strictly positive guiding function $\psi_G(\mathbf{R})$ whose role is to modify the random walk, while an antisymmetric trial function $\psi_T(\mathbf{R})$ that should resemble the solution as closely as possible is used to project out quantities of interest, such as the local energy E_T. Thus the density of walkers (5) generated by the walk will be

$$
f(\mathbf{R},\tau) = \psi_G(\mathbf{R})\psi(\mathbf{R},\tau) \underset{\tau\to\infty}{\longrightarrow} \psi_G(\mathbf{R})\phi_0(\mathbf{R}) \qquad (9)
$$

while the energy estimator (8) after equilibration is now

$$
E_0 = \frac{\sum_m^{N_w} \frac{\hat{H}\psi_T(\mathbf{R_m})}{\psi_G(\mathbf{R_m})}}{\sum_m^{N_w} \frac{\psi_T(\mathbf{R_m})}{\psi_G(\mathbf{R_m})}}. \qquad (10)
$$

We separate now the set $\{\mathbf{R_m}\}$ of walkers into two subsets of walkers $\{\mathbf{R}_m^+\}$, $\{\mathbf{R}_m^-\}$ that respectively add or subtract their contributions to statistical expectations such as (10), which becomes

$$
E_0 = \frac{\sum_m^{N_p} \left[\frac{\hat{H}\psi_T(\mathbf{R}_m^+)}{\psi_G(\mathbf{R}_m^+)} - \frac{\hat{H}\psi_T(\mathbf{R}_m^-)}{\psi_G(\mathbf{R}_m^-)}\right]}{\sum_m^{N_p} \left[\frac{\psi_T(\mathbf{R}_m^+)}{\psi_G(\mathbf{R}_m^+)} - \frac{\psi_T(\mathbf{R}_m^-)}{\psi_G(\mathbf{R}_m^-)}\right]} \qquad (11)
$$

where N_p is the number of pairs of configurations that enter the averaging. If the signed walkers independently sample the configuration space according to the distribution (9) they will lead to the fermion decay. In particular the denominator of Eq. (11) will be unstable since the $\{\mathbf{R}_m^+\}$ and the $\{\mathbf{R}_m^-\}$ will be equally (symmetrically) distributed, averaging their contributions around zero.

The incorporation of a correlation between pairs of walkers in the random-walk process has been shown to be effective in avoiding this decay of the signal-to-noise ratio that regularly occurs in a fermionic DMC[8,9]. Before introducing correlation, we first start by distinguishing the signed walkers by means of different ψ_G's which we call $\psi_G^{\pm}$ respectively.

C. The Guiding Functions

The usual role of a guiding function in a Diffusion Monte Carlo scheme is that of importance sampling in configuration space, thus allowing a more efficient calculation. In FMC we introduce two functions $\psi_G^{\pm}$ which bias differently the populations of plus and minus walkers and thus act as symmetry breaking fields.

The ingredients of our guiding functions are the usual ones for Quantum Monte Carlo studies of many-body systems: Slater Determinants $D^{\uparrow(\downarrow)}$ of like-spin single particle wavefunctions, and two symmetric Jastrow products, $J^S(\mathbf{R})$ and $J^A(\mathbf{R})$ with different parameters.

We now construct a function antisymmetric under permutation of atom labels

$$
\psi_A(\mathbf{R}) = J^A(\mathbf{R})D^{\uparrow}(\mathbf{R})D^{\downarrow}(\mathbf{R}) \qquad (12)
$$

and a symmetric one

$$
\psi_S(\mathbf{R}) = J^S(\mathbf{R}) \qquad (13)
$$

Finally, the guiding functions themselves are constructed by combining (12) and (13):

$$
\psi_G^{\pm}(\mathbf{R}) = \sqrt{\psi_S^2(\mathbf{R}) + c^2\psi_A^2(\mathbf{R})} \pm c\psi_A(\mathbf{R}) \qquad (14)
$$

with c a small and adjustable parameter. The functions $\psi_G^{\pm}$ are positive for any $\mathbf{R}$, as is necessary for an importance function.

For an odd permutation $\mathcal{P}$ of particles in a configuration $\mathbf{R}$, one has

$$
\psi_G^{\mp}(\mathcal{P}\mathbf{R}) = \psi_G^{\pm}(\mathbf{R}) \qquad (15)
$$

so that the biased distributions of the two signed walkers map into each other.

In the limit of small c, the functions $\psi_G^{\pm}(\mathbf{R})$ are dominated by ψ_S so that $\mathbf{R}^+$ and $\mathbf{R}^-$ are then preferentially drifted towards each other.

The orbitals of our Slater determinants are

$$
\chi_{\mathbf{r_i}}^{\mathbf{k}} = e^{i\mathbf{k}\cdot\left[\mathbf{r_i}+\lambda_B\sum_{\mathbf{j}\neq\mathbf{i}}\eta(\mathbf{r_{ij}})\mathbf{r_{ij}}\right]} \qquad (16)
$$

with η the standard backflow function[10]

$$
\eta(r) = \left(\frac{r-R_B}{R_B}\right)^{m_B} \exp\left\{-\left[\frac{r-S_B}{\omega_B}\right]^{n_B}\right\} \qquad (17)
$$

and the Jastrow products are

$$J^{A,S}(\mathbf{R}) = \exp\left[-\sum_{i<j} u(r_{ij}) - \frac{\lambda_t^{A,S}}{2}\sum_l \mathbf{G}(l)\cdot\mathbf{G}(l)\right], \tag{18}$$

providing two-body correlations via a pseudopotential of the McMillan type

$$u(r) = \frac{1}{2}\left(\frac{b^{A,S}}{r}\right)^{m^{A,S}} \tag{19}$$

and the three-body correlations via the "triplet" term

$$\mathbf{G}(l) = \sum_{i\neq l} \xi(r_{li})\mathbf{r_{li}} \tag{20}$$

with

$$\xi(r) = \left(\frac{r-R_t}{R_t}\right)^{m_t^{A,S}} \exp\left[-\left(\frac{r-S_t^{A,S}}{\omega_t^{A,S}}\right)^{n_t^{A,S}}\right]. \tag{21}$$

R_B and R_t in the long range factors of (17) and (21) respectively, are cut-off lengths set equal to half of the simulation box size l

$$\frac{l}{2} = \frac{1}{2}\left(\frac{N}{\rho}\right)^{\frac{1}{3}} \tag{22}$$

with ρ the density of the system. λ_B and $\lambda_t^{A,S}$ (strengths), S_B and $S_t^{A,S}$ (centers of the Gaussians), ω_B and $\omega_t^{A,S}$ (widths of the Gaussians), $m^{A,S}, m_t^{A,S}, n_t^{A,S}, m_B, n_B$ are other optimized parameters.

The diffusion process described by Eq. (6) for the distribution (9), is generalized as follows: the two $\psi_G^{\pm}$ are applied separately to drift the walkers of a pair from their old positions $\mathbf{R}_o^+, \mathbf{R}_o^-$:

$$\mathbf{R}_d^{\pm} = \mathbf{R}_o^{\pm} + 2\delta\tau\frac{\nabla\psi_{\mathbf{G}}^{\pm}(\mathbf{R}_o^{\pm})}{\psi_G^{\pm}(\mathbf{R}_o^{\pm})}. \tag{23}$$

In addition, while the standard DMC algorithm would have the configurations diffuse independently, we introduce correlation into the process.

D. Reflected Correlated Dynamics

The motivation for introducing a correlation among the random-walks is that of controlling the growth of the symmetric ground state with respect to the fermionic state. We use the cancellation methods first introduced by Arnow *et al.*[11]. But this cancellation, which involves subtracting the Green's functions of the plus and minus walkers, has a range of about the square root of the time step. Walkers must come within this range for the cancellation to be effective, and in many dimensions, the chance that two walkers will do so is exponentially small. As pointed out by Liu, Zhang, and Kalos[9], appropriate correlation among walkers can ensure efficient cancellation.

In particular, we will consider pairs with their Gaussians correlated as follows: one vector, say $\mathbf{U}^+$ for the plus walker, is generated in the usual way for one of the walkers, that is as a vector $\mathbf{U}^+$ with $3N$ Gaussian random variables each of mean zero and variance $\delta\tau$. The other vector $\mathbf{U}^-$ is obtained by reflection in the perpendicular bisector of the line segment $\mathbf{R}_d^+ - \mathbf{R}_d^-$.

This choice of correlation[12] guarantees the meeting of the two components of a pair in any number of dimensions, so that cancellation is efficient.

It is important to point out[12] that the marginal dynamics of either walker is, except for cancellation, the same on the average as that of a free one walkers, guaranteeing that averages over the walks are unbiased.

The diffusion steps $\mathbf{U}^+$ of $\mathbf{R}_d^+$ and $\mathbf{U}^-$ of $\mathbf{R}_d^-$ are described by

$$\begin{aligned}\mathbf{R}_n^+ &= \mathbf{R}_d^+ + \mathbf{U}^+\\ \mathbf{R}_n^- &= \mathbf{R}_d^- + \mathbf{U}^-\end{aligned} \tag{24}$$

where

$$\mathbf{U}^- = \mathbf{U}^+ - 2\left(\mathbf{U}^+\cdot\frac{\mathbf{R}_d^+ - \mathbf{R}_d^-}{|\mathbf{R}_d^+ - \mathbf{R}_d^-|}\right)\cdot\frac{\mathbf{R}_d^+ - \mathbf{R}_d^-}{|\mathbf{R}_d^+ - \mathbf{R}_d^-|}. \tag{25}$$

Seen as a whole, the short time approximation to the Green's function that solves the diffusive part of Eq. (6) advancing the single walker from an old position $\mathbf{R}_o$ to a new one $\mathbf{R}_n$ by taking the drift (23) and the diffusion (24) steps, is

$$G(\mathbf{R}_n^{\pm} \leftarrow \mathbf{R}_o^{\pm}, \delta\tau) = \frac{e^{-\frac{1}{(2\delta\tau)}\left[\mathbf{R}_n^{\pm} - \mathbf{R}_o^{\pm} - \frac{\nabla\psi_G^{\pm}(\mathbf{R}_o^{\pm})}{\psi_G^{\pm}(\mathbf{R}_o^{\pm})}\right]}}{(2\pi\delta\tau)^{3N/2}} \tag{26}$$

while the absorbtion rate equation nature of Eq. (6) is accounted for by the branching stage that follows.

E. Branching of Pairs

For each pair, the branching of a walker is correlated with the behavior of its partner via a ratio r_g of the Gaussians that explicitly takes into account the possibility of an overlap of the future positions of the walkers of the pair, as shown in Fig. (1) r_g is given by

$$r_g(\mathbf{R}_n^{\pm} \leftarrow \mathbf{R}_o^{\pm}, \mathbf{R}_o^{\mp}) = \frac{\exp\left[-\frac{(\mathbf{R_n^{\pm}} - \mathbf{R_o^{\mp}})}{2\delta\tau}\right]}{\exp\left[-\frac{(\mathbf{R_n^{\pm}} - \mathbf{R_o^{\pm}})}{2\delta\tau}\right]}, \tag{27}$$

and is a measure of the cancellation degree for the pair. It is straightforward to prove that

$$r_g(\mathbf{R}_n^+ \leftarrow \mathbf{R}_o^+, \mathbf{R}_o^-) = r_g(\mathbf{R}_n^- \leftarrow \mathbf{R}_o^-, \mathbf{R}_o^+). \tag{28}$$

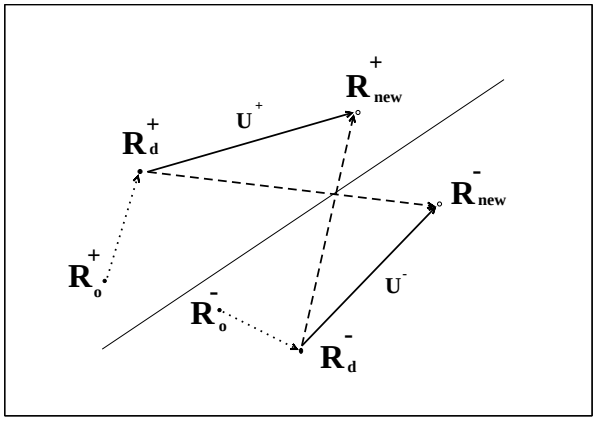

FIG. 1: Scheme of reflected correlated dynamics. The diffusion step U^- is built by reflecting U^+ with respect to the perpendicular bisector of the line segment $\mathbf{R}_d^+ - \mathbf{R}_d^-$. The branching of the new walkers $\mathbf{R}_n^+, \mathbf{R}_n^-$ will reflect the relative probability of diffusing to each other's new position in the configuration space (as suggested by the dashed lines). Dotted lines represent the drift step.

When the two walkers of a pair have the same probability of moving to the same new position their future contributions at that point cancel. By introducing the ratio (27) one removes these unproductive walkers from the population.

We introduce the generalization of the usual branching factor:

$$B^{\pm}(\mathbf{R}^{\pm}) = e^{-\delta\tau\left[E_L(\mathbf{R}^{\pm})-E_T\right]} \tag{29}$$

where the local energy (7) is now calculated by using one of the two guiding functions,

$$E_L(\mathbf{R}^{\pm}) = \frac{\hat{H}\psi_G^{\pm}(\mathbf{R}^{\pm})}{\psi_G^{\pm}(\mathbf{R}^{\pm})}. \tag{30}$$

The branching weight for each walker in the pair now becomes:

$$\omega(\mathbf{R}^{\pm}) = B^{\pm}(\mathbf{R}^{\pm}) \max\left[0, 1 - \frac{B_x^{\pm}(\mathbf{R}^{\pm})}{B^{\pm}(\mathbf{R}^{\pm})} r_g \frac{\psi_G^{\pm}(\mathbf{R}^{\pm})}{\psi_G^{\mp}(\mathbf{R}^{\pm})}\right] \tag{31}$$

where a "crossing local energy" and a "crossing branching factor" have been defined respectively as:

$$E_L^x(\mathbf{R}^{\pm}) = \frac{\hat{H}\psi_G^{\mp}(\mathbf{R}^{\pm})}{\psi_G^{\mp}(\mathbf{R}^{\pm})} \tag{32}$$

$$B_x^{\pm}(\mathbf{R}^{\pm}) = e^{-\delta\tau\left[E_L^x(\mathbf{R}^{\pm})-E_T\right]}. \tag{33}$$

Eq. (31) accounts for the fact that, when a walker is in the region where it contributes more, one has $\psi_G^{\pm}(\mathbf{R}^{\pm})$ greater than $\psi_G^{\mp}(\mathbf{R}^{\pm})$ and the weight is then close to $B^{\pm}$. The presence of the "max" in the expression for $\omega(\mathbf{R}^{\pm})$ assures that when the difference of Green's functions at a point is positive, then only plus walkers can be generated there (and similarly for minus walkers.)

The factors $\omega(\mathbf{R}^{\pm})$ are used for weighting contributions of the walkers to averaged quantities, while N_m copies of the pair $\{\mathbf{R}_m^+, \mathbf{R}_m^-\}$ are advanced together to the next step, where

$$N_m = int[\omega^p + \mathcal{U}_{[0,1]}] \tag{34}$$

where $\mathcal{U}_{[0,1]}$ is a random number uniformly distributed between 0 and 1, and

$$\omega^p = \min[\omega(\mathbf{R}^+), \omega(\mathbf{R}^-)]. \tag{35}$$

The difference between the weights of the two walkers is retrieved in a "repairing" step, described in the next section. It is evident that when for a pair $r_g = 1$ (i.e. overlapping oppositely-signed walkers $\mathbf{R}^+ = \mathbf{R}^-$), the weight ω^p of the pair, and thus the number of its children, will be zero.

F. Repairing

Our method comprises a random walk of pairs of signed walkers. For it to be unbiased, all weights $\omega(\mathbf{R}^{\pm})$ generated in Eq. (31) must be reflected in walkers included in the population. As indicated above, some weight, $\max[\omega(\mathbf{R}^+), \omega(\mathbf{R}^-)] - \min[\omega(\mathbf{R}^+), \omega(\mathbf{R}^-)]$ is lost in generating new pairs. That is retrieved by "repairing", that is by generating a new pair using the walker whose weight is larger and an odd permutation $\mathcal{P}$ of like-spin particles applied to that walker. Since each of these walkers contributes exactly the same amount to any quantity projected with an antisymmetric test function, we must apply another factor of one half. That is,

$$\mathbf{R}_{ad}^{\mp} = \mathcal{P}\mathbf{R}_{ad}^{\pm} \tag{36}$$

$$\mathbf{R}_{ad}^{\pm} \longrightarrow \{\mathbf{R}_{ad}^+, \mathbf{R}_{ad}^-\}. \tag{37}$$

The permutation $\mathcal{P}$ is taken to be that pair exchange of like-spin particles that minimizes the Euclidean distance between the original and permuted walkers. $N_{repaired}$ copies of the new pair is then forwarded to the next time step, with

$$N_{repaired} = int[\omega^{diff} + \mathcal{U}_{[0,1]}] \tag{38}$$

where

$$\omega^{diff}(\mathbf{R}_n^+, \mathbf{R}_n^-) = 0.5\left[\omega(\mathbf{R}_{ad}) - \omega(\mathbf{R}^{\mp})\right]. \tag{39}$$

G. Projection

Quantities of interest, such as the total energy, are projected out by using a trial wave function. In our FMC

method that role is played by the antisymmetric function ψ_A of Eq. (12). To account for the branching process, each pair may contribute once weighted with $\omega(\mathbf{R}_m^{\pm})$ of Eq. (31). Eq. (11) then becomes:

$$E_0 = \frac{\sum_m^{N_p} \left[\frac{\hat{H}\psi_A(\mathbf{R}_m^+)}{\psi_G(\mathbf{R}_m^+)} \omega(\mathbf{R}_m^+) - \frac{\hat{H}\psi_A(\mathbf{R}_m^-)}{\psi_G(\mathbf{R}_m^-)} \omega(\mathbf{R}_m^-) \right]}{\sum_m^{N_p} \left[\frac{\psi_A(\mathbf{R}_m^+)}{\psi_G(\mathbf{R}_m^+)} \omega(\mathbf{R}_m^+) - \frac{\psi_A(\mathbf{R}_m^-)}{\psi_G(\mathbf{R}_m^-)} \omega(\mathbf{R}_m^-) \right]}. \quad (40)$$

Alternatively one can count multiple children walkers each with weight one.

To this energy a constant value due to the tail correction of the potential is then added for each walker contributing to the averaging.

H. Acceptance/Rejection

Acceptance/Rejection algorithms have been shown to improve convergence in Monte Carlo algorithms[5]. For diffusion Monte Carlo, this improvement achieves an error of second order in the time step. Use of the simple short-time Green's function is first order.

1. *Weight-correlated Acceptance/Rejection scheme*

The likelihood Q of a move to a new position in the configuration space $\mathbf{R}_o^{\pm} \to \mathbf{R}_n^{\pm}$ for each of the two walkers of a pair is given by the ratio of the $\mathbf{R}_n^{\pm} \to \mathbf{R}_o^{\pm}$ back-diffusion Gaussian to the $\mathbf{R}_o^{\pm} \to \mathbf{R}_n^{\pm}$ forward-diffusion Gaussian, multiplied by the ratio of the intensities of the guiding function in the new and old position:

$$Q(\mathbf{R}_o^{\pm} \to \mathbf{R}_n^{\pm}) = \frac{|\psi_G^{\pm}(\mathbf{R}_n^{\pm})|^2}{|\psi_G^{\pm}(\mathbf{R}_o^{\pm})|^2} \frac{e^{-\left[\mathbf{R}_o^{\pm} - \mathbf{R}_n^{\pm} - \frac{\nabla\psi_G^{\pm}(\mathbf{R}_n^{\pm})}{\psi_G^{\pm}(\mathbf{R}_n^{\pm})}\right]}}{e^{-\left[\mathbf{R}_n^{\pm} - \mathbf{R}_o^{\pm} - \frac{\nabla\psi_G^{\pm}(\mathbf{R}_o^{\pm})}{\psi_G^{\pm}(\mathbf{R}_o^{\pm})}\right]}} \quad (41)$$

for which the acceptance probability of the move would be

$$A(\mathbf{R}_o^{\pm} \to \mathbf{R}_n^{\pm}) = \min[1, Q] \quad (42)$$

meaning that if $A \geq \mathcal{U}_{[0,1]}$ the move to the new position is accepted, while if $A < \mathcal{U}_{[0,1]}$ the move is rejected and the old position is used again as the new one.

The weight associated with the accepted walker is then given by Eq. (31). On the contrary, in case of rejection, the old walker is associated with weight one.

Besides this scheme, adapted from standard DMC codes to our correlated pairs, for which the correlation enters just in the weight of the accepted/rejected walker, we added, consistent with the correlated walker scheme, a dynamic-correlated acceptance-rejection, which is described in the next section.

In order to avoid wasting unnecessary computer cycles, this modification is carried out only when the ratio (27) of their Gaussian steps is of considerable magnitude (at least 10^{-2}).

2. *Dynamic-correlated Acceptance/Rejection scheme*

In order to include the "cancellation" of the opposite-sign partner in the acceptance of a walker move, in the same fashion as in Eq. (41) we introduce a "crossing acceptance probability", i.e. the probability of the minus(plus) walker to arrive at the same position as the plus(minus) partner, by calculating

$$Q_x(\mathbf{R}_o^{\mp} \to \mathbf{R}_n^{\pm}) = \frac{|\psi_G^{\mp}(\mathbf{R}_n^{\pm})|^2}{|\psi_G^{\mp}(\mathbf{R}_o^{\mp})|^2} \frac{e^{-\left[\mathbf{R}_o^{\mp} - \mathbf{R}_n^{\pm} - \frac{\nabla\psi_G^{\pm}(\mathbf{R}_n^{\pm})}{\psi_G^{\pm}(\mathbf{R}_n^{\pm})}\right]}}{e^{-\left[\mathbf{R}_n^{\pm} - \mathbf{R}_o^{\mp} - \frac{\nabla\psi_G^{\mp}(\mathbf{R}_o^{\mp})}{\psi_G^{\mp}(\mathbf{R}_o^{\mp})}\right]}} \quad (43)$$

for which the acceptance probability would be

$$A_x(\mathbf{R}_o^{\mp} \to \mathbf{R}_n^{\pm}) = \min[1, Q_x] \quad (44)$$

In this case, Eq. (31) becomes

$$\omega^{\pm}(\mathbf{R}_n^{\pm}) = B^{\pm}(\mathbf{R}_n^{\pm}) \max\left[0, 1 - \frac{A_x}{A} \frac{B_x^{\pm}(\mathbf{R}_n^{\pm})}{B^{\pm}(\mathbf{R}_n^{\pm})} r_g \frac{\psi_G^{\pm}(\mathbf{R}^{\pm})}{\psi_G^{\mp}(\mathbf{R}^{\pm})}\right] \quad (45)$$

3. *Age-dependent Acceptance*

Persistent walkers are those in deep local minima in the sampling function so that they move away with very small probability. To avoid the effect of long-standing stale configurations in the Acceptance/Rejection algorithm, an age-enforced acceptance factor has been proposed by Umrigar, Nightingale and Runge[13]. This consists in noting the history of a walker, eventually raising its acceptance probability if it has not been moved after some given number of steps ("*agemax*"). The acceptance probability Eq. (42) is increased by a factor

$$A_0 e^{(age - agemax)} \quad (46)$$

where *age* is the number of steps for which the walker did not change its position and A_0 is an adjustable parameter.

I. Second-Stage Importance Sampling

In analogy to the concept of importance sampling[14], we introduce "Second Stage Importance Sampling" (SSIS) to improve the efficiency of the method.

The optimum importance function gives the expected contribution– here of a walker pair– to the quantity of interest– here the overlap with an antisymmetric test function. Clearly this is not completely captured by the functions $\psi_G^{\pm}$ that we have introduced to guide the walkers. They do not show any dependence on the separation of $\mathbf{R}^+$ and $\mathbf{R}^-$ which is important in the cancellation process, or any other joint dependence on the positions of the walkers. We therefore introduce the possibility of using an arbitrary function $f(\mathbf{R}^+, \mathbf{R}^-)$ to account for the full importance, and include an extra branching process based on ratios of f before and after a time step. Let

$$\omega^p \rightarrow \omega^p \frac{f_n^S}{f_o^S} \tag{47}$$

$$\omega^{diff} \rightarrow \omega^{diff} \frac{f_n^S}{f_o^S} \tag{48}$$

where f_o^S and f_n^S are the SSIS functions respectively for the old and new position of the pair. The new weights thus obtained are used in order to determine the number of replicas of the pair as in (34) and of the repaired walker as in (38), while the factor $1/f_o^S$ alone is used with the weights in (40), in order to "unweight" the contribution brought by the pair in the previous step. We experimented with two different forms.

1. *Denominator-weighted sampling*

In a first version of the SSIS, an S-shaped function of the pair's denominator $\mathcal{D}$, namely

$$f_1^S(\mathbf{R}_o^+, \mathbf{R}_o^-) = (1-\epsilon)\left(\frac{\mathcal{D}-\bar{\mathcal{D}}}{\sqrt{(\mathcal{D}-\bar{\mathcal{D}})^2+\Delta\mathcal{D}^2}}\right)+1 \tag{49}$$

where $\bar{\mathcal{D}}$ is approximately the average denominator for a pair, ϵ a small quantity and $\Delta\mathcal{D}$ the width of a range of significant values for $\mathcal{D}$. This function works in the following way: if a pair improves the value of its contribution to the energy denominator, $\mathcal{D}$, with respect to the previous step, its branching weight is increased by a factor proportional to the ratio of the values of this function.

2. *Euclidean-distance sampling*

A second version of SSIS measures the Euclidean distance between the walkers of each pair in the $3N$-dimensional space of the configurations:

$$f_2^S(\mathbf{R}^+, \mathbf{R}^-) = \left[\sum_{i=1}^{3N}(x_i^+ - x_i^-)^2\right]^{\frac{1}{2}} \tag{50}$$

Thus walkers that move apart will branch more than walkers that come together reflecting their smaller likelihood of cancellation.

III. RESULTS

A. Common things about the runs

We developed a MPI-parallelized Fortran code that runs on IBM SP machines. Most of the runs were made with 192 pairs of walkers distributed among 16 processors. At each step the distribution of pairs was rebalanced among the processors.

In order to simulate bulk ^{3}He at zero temperature we considered 54 atoms with periodic boundary conditions at the equilibrium density $0.273\sigma^{-3}$, where σ is the "Aziz" unit ($\sigma = 2.556\mathring{A}$). The interaction used was the HFDHE2 Aziz potential[15].

The experimental energy[16] for liquid-^{3}He at the equilibrium density is -2.47 ± 0.01 K per atom.

B. Analysis tools

We express the length of a run in terms of the ratio of the root mean square of the diffusion length of a particle to the mean spacing r between particles[17]

$$q = \frac{\sqrt{3\frac{\hbar^2}{2m}\delta\tau N_{steps}}}{r_{He^3-He^3}} \tag{51}$$

where $\delta\tau$ is the length of a step in imaginary time. When q equals one, $N_{steps}\delta\tau$ corresponds to a relaxation time, τ_{rel}. Thus the lengths of runs in what follows will be generally expressed as multiples of this relaxation time and it is normally assumed that the calculation is equilibrated after one relaxation time at which point we will start to gather statistics.

As an example, for a time step of $6 \times 10^{-5}\ K^{-1}$, τ_{rel} would be reached after about 9.5×10^4 steps assuming 100 % acceptance).

Another measure of relaxation time uses the energy gap between the symmetric state to which the common DMC algorithm spontaneously evolves and the antisymmetric state we seek. For He systems the difference in energy between the ^{3}He (E_a) and the ^{4}He (E_s) cases is $1K$ per particle. Then for our 54 particles system

$$\tau_{rel} \simeq \frac{1}{E_s - E_a} = \frac{1}{54K} = 0.0185K^{-1} \tag{52}$$

As an example, with a time step of $6 \times 10^{-5}\ K^{-1}$, the last relaxation amounts to about 300 steps. This would be the valid range in which one could perform a transient estimation calculation.

Because the denominator is not always positive, a great deal of care is needed to perform reasonable statistical analysis. We have relied on reblocking into large groups and sought errors that are independent of the blocking and when the block denominators are large and positive.

C. Stability

In analyzing the stability we refer to the "cumulative denominator" of the calculations, which is the sum of the contributions of each pair of walkers to the denominator of the local energy (11) over the steps, so that at a given step the partial denominator will be

$$\mathcal{D} = \sum_{m=1}^{N_p} \left[\frac{\psi_A(\mathbf{R}_m^+)}{\psi_G^+(\mathbf{R}_m^+)} \omega(\mathbf{R}_m^+) - \frac{\psi_A(\mathbf{R}_m^-)}{\psi_G^-(\mathbf{R}_m^-)} \omega(\mathbf{R}_m^-) \right] \quad (53)$$

where N_p is the number of pairs of walkers. When walkers are in favorable pockets, $\mathcal{D}$ will be positive, and the sum of $\mathcal{D}$'s over the steps (the "cumulative denominator") will be a growing function of time. By setting $c = 0$ in $\psi_G^{\pm}$, i.e. annihilating the antisymmetric contribution in the importance sampling functions, we restore the symmetry between plus and minus walkers and restore the usual signal to noise decay.

We have investigated the stability of the calculations with respect to the "mixing" factor c which determines the amount of asymmetry introduced in the guiding functions.

Cumulative denominators are shown in Fig. 2 for different values of c. The runs are stable in the long term for a wide range of c, spanning orders of magnitudes ($10^{-23} - 10^{-22}$). Demonstrating stability for a much smaller value of c (10^{-25}) presumably needs a longer run. On the other hand, it could seem strange that for a bigger c, namely (10^{-21}) the run is not stable as one might expect, in which case we should recover the fixed node limit. This is due to the enhanced role taken by the zeros of the antisymmetric part of the guiding function that leads to uncontrolled numbers for walkers close to the nodes of the antisymmetric part. This also explains some big fluctuations in runs with c smaller but still affected by the nodes of ψ_A. One could presumably cure this by devising better guiding functions.

D. Eigenvalues

In discussing the results of our code for the eigenvalues, it is important to remember that the current method suffers from a dependence on population size that is much larger than in standard DMC. The reason for this lies in the fact that branching is determined primarily by the local energy of the guiding functions, $\psi_G^{\pm}$. These are not good approximations to eigenfunctions, in complete

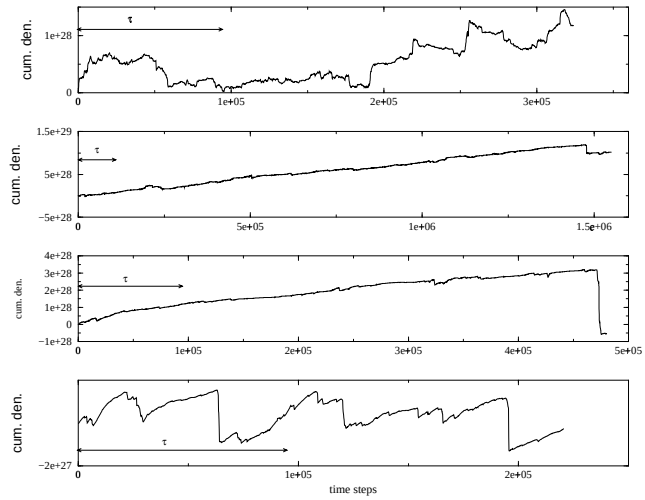

FIG. 2: Stability of the FMC runs for different values of the *mixing* factors c. From top to bottom: $c = 10^{-25}, 10^{-23}, 10^{-22}, 10^{-21}$. Fluctuations for big c are due to an increasing importance of the nodes of ψ_A, while fluctuations for small c indicate cancellation between contributions of $\mathbf{R}^{\pm}$. Acceptance/Rejection but no SSIS have been included in all these runs.

TABLE I: FMC results with respect to parameters used. Note that no extrapolation to zero time step has been calculated. Bottom line: fixed node result.

N_p	c	$\delta\tau$ in K^{-1}	A/R	$SSIS$	length in τ_{rel}	$E(\Delta E)$ in K
192	10^{-23}	6×10^{-5}	yes	denom	16	-2.24(3)
192	10^{-23}	6×10^{-5}	yes	no	20	-2.26(13)
192	10^{-22}	6×10^{-5}	yes	eucl	11	-2.215(12)
192	10^{-22}	6×10^{-5}	no	denom	25	-2.24(14)
192	10^{-22}	6×10^{-5}	yes	denom	25	-2.38(3)
192	FXN	6×10^{-5}	yes	denom	10	-2.369(2)

contrast to DMC. If all walkers had a multiplicity of exactly unity, then only one walker would be needed; the population-size bias increases with the variance in the branching multiplicity. The runs reported here have a rather small average population of 192 pairs.

Table I shows average results for the various runs. In particular it is shown that even with a small population of 192 pairs, a long FMC run with SSIS and Acceptance/Rejection procedure gives results that are comparable with the fixed node ones.

E. Dependance on ψ_G parameters

It is well known that the quality of Quantum Monte Carlo computations are strongly dependent upon the quality of the trial wavefunctions. The results of our FMC method, though theoretically independent of the ψ_T and ψ_G, presently shows substantial dependence on the accuracy of the trial and guiding wavefunctions.

Parameters used in the symmetric and antisymmetric

TABLE II: Parameters used in the guiding and trial wave functions.

Jastrow 2-body		b	m			
ψ_A		1.15	5			
ψ_S		1.15	5			
Jastrow 3-body	R_t	λ_t	S_t	ω_t	m_t	n_t
ψ_A	2.87	-12	0.85	0.5	3	2
ψ_S	2.87	0	0.85	0.5	3	2
Backflow	R_B	λ_B	S_B	ω_B	m_B	n_B
ψ_A	2.87	1	0.85	0.5	3	2

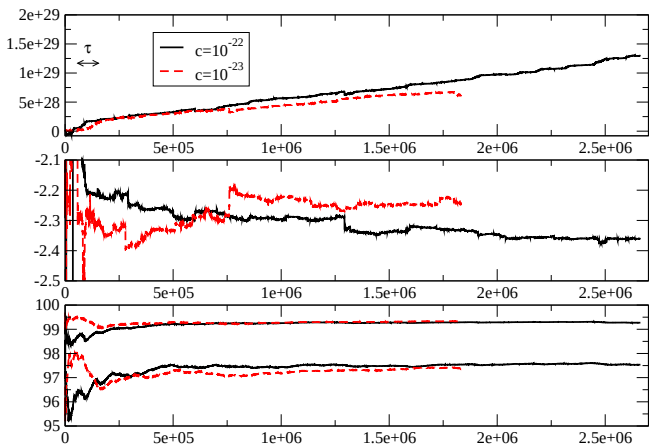

FIG. 3: Effect of the amount of antisymmetry in the guiding function. Top: cumulative denominator; Center: cumulative energy; Bottom: cumulative acceptances for $\mathbf{R}^+, \mathbf{R}^-$. This runs have been obtained with Acceptance/Rejection, denominator-weighted SSIS and $\delta\tau = 6 \times 10^{-5}$.

terms of the guiding function are shown in Table II.

The parameter c governs the degree of antisymmetry in the guiding functions.

In Fig. 3 we compare two runs that differ only by the value assigned to c, and share all the other features, like the inclusion of Acceptance/Rejection and SSIS-denom. procedures.

F. Effect of Second Stage Importance Sampling

1. *Denominator-weighted sampling*

For the parameters appearing in the function (49) we generally took $\epsilon = 0.1$, $\bar{\mathcal{D}}$ as the average denominator in a long run without SSIS and $\Delta\mathcal{D}$ as two times $\bar{\mathcal{D}}$. Fig. 4 shows the same calculation performed with and without SSIS. Both the runs have been obtained with

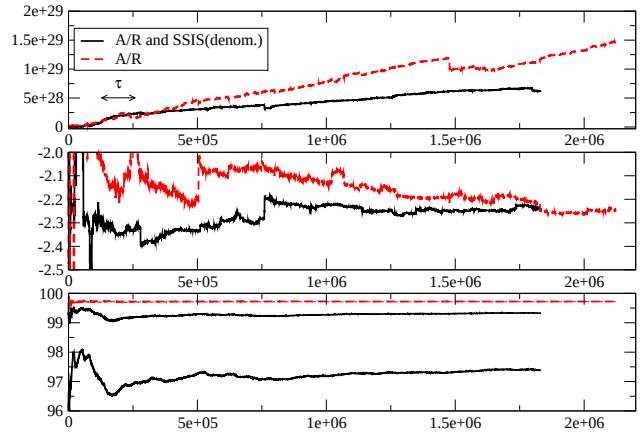

FIG. 4: Effect of the SSIS-denom. on the calculation. Top: cumulative denominator; Center: cumulative energy; Bottom: cumulative acceptances for $\mathbf{R}^+, \mathbf{R}^-$ (they coincide for the non-SSIS run). These runs have been obtained with denominator-weighted SSIS, $\delta\tau = 6 \times 10^{-5}$ and $c = 10^{-23}$.

$c = 10^{-23}$ and applying Acceptance/Rejection. The presence of SSIS introduces a difference between the $\mathbf{R}^+, \mathbf{R}^-$ acceptances that remains to be explained. Extrapolation of energy data for these runs gives $-2.26(13)K$ (A/R only) and $-2.24(3)K$ (A/R and SSIS), indicating that this form of SSIS is indeed more efficient.

2. *Euclidean-distance sampling*

Fig. 5 shows the same calculation performed with and without SSIS. Both runs have been obtained by applying acceptance/rejection, and use the same time-step. but different c values: ($c = 10^{-23}$ without SSIS, $c = 10^{-22}$ with SSIS). Extrapolation of energy data for these runs gives $-2.26(13)K$ (A/R only) and $-2.215(12)K$ (A/R and SSIS), indicating that in this case too, if we take in consideration the lengths of the runs, the presence of SSIS tends to improve the efficiency.

A comparison between calculations which differ only in the SSIS functions is shown in Fig. 6. The disparity in length does not allow a definitive comparison. Nevertheless the Euclidean-distance sampling seems to improve the efficiency in the accumulation of the denominator, reducing at the same time the overall acceptance ratio. It is worth noticing that both SSIS functions generate a gap in the acceptance ratios for positive and negative walkers. Though the runs share the same parameters ($c = 1 \times 10^{-22}$, $\delta\tau = 6 \times 10^{-5}$) the denom-SSIS one yields too a much better estimate for the eigenvalue, $-2.38(3)$ vs. $-2.215(12)$.

G. Effect of Acceptance-Rejection

Fig. 7 shows the same calculation performed with and without Acceptance/Rejection. Stability of the denomi-

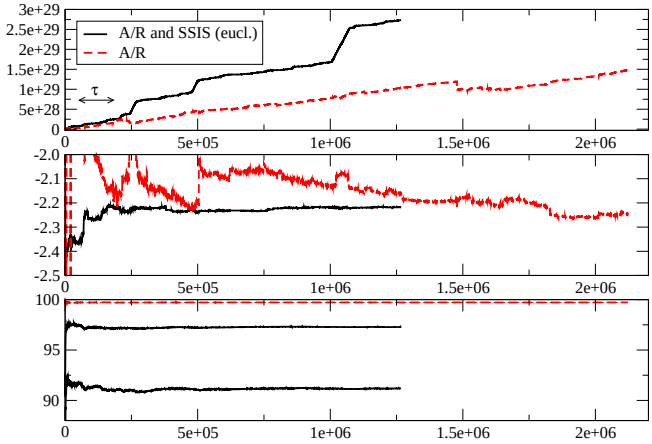

FIG. 5: Effect of the SSIS-eucl. on the calculation. Top: cumulative denominator; Center: cumulative energy; Bottom: cumulative acceptances for $\mathbf{R}^+, \mathbf{R}^-$ (they coincide for the non-SSIS run). This runs have been obtained with Euclidean distance SSIS, $\delta\tau = 6 \times 10^{-5}$ and $c = 10^{-23}$ (A/R-only run) and $c = 10^{-22}$.

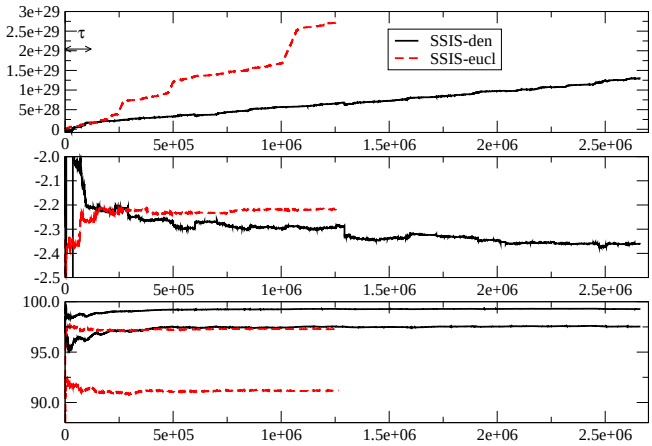

FIG. 6: Same run repeated with different SSIS functions. Top: cumulative denominator; Center: cumulative energy; Bottom: cumulative acceptances for $\mathbf{R}^+, \mathbf{R}^-$. This runs have been obtained with $c = 1 \times 10^{-22}$ and $\delta\tau = 6 \times 10^{-5}$.

nator is good in both cases (SSIS-denom has been used), but the run without A/R suffered substantial fluctuations in the partial energy, complicating the reblocking procedure, but yielded $-2.24(14)K$, whereas the A/R procedure gives less fluctuations and a much better estimate $-2.38(3)K$.

We have to note that the event of a dynamic-correlated acceptance has been in general very rare.

A result that emphasizes the difference between the usual DMC method and ours is that stale configurations show up regularly as a common feature of our simula-

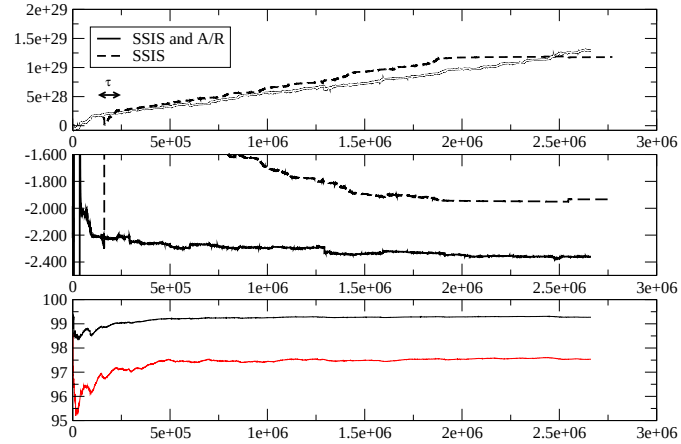

FIG. 7: Effect of the Acceptance/Rejection procedure on the calculation. Both runs included the SSIS-denom. function. Top: cumulative denominator; Center: cumulative energy; Bottom: cumulative acceptances (for the A/R run only), $\mathbf{R}^+$ (solid), $\mathbf{R}^-$ (dotted) The two runs share the same parameters for ψ_G (in particular, $c = 10^{-22}$) and have been obtained with $\delta\tau = 2 \times 10^{-5}$ (SSIS only) and $\delta\tau = 6 \times 10^{-5}$ (SSIS with A/R, respectively).

tions, with ages easily reaching 80-100 steps, while it has been noted[13] that in DMC studies of molecules ages rarely reached 40 steps and thus the acceptance probability enhancing procedure described in Sec. (II H 3) never occurred. Parameters in factor (46) used in our work and in[13] are the same: $A_0 = 1.10, agemax = 50$. We observe that the occurance of persistent walkers is usually avoided in DMC by reverting to small time steps. Moreover, in DMC calculations stale configurations disappear in the limit of $\psi_G = \phi_0$, a limit that has to be excluded *a priori* for our ψ_G's to maintain stability. It is then evident from our results, that for FMC, even for very short time steps like the ones used here, walkers can be trapped and thus the age-enforced procedure should be regarded as an essential part of the procedure.

H. Interplay between A/R and SSIS

It is clear from the plots that both Acceptance/Rejection and SSIS help in preventing large fluctuations and in stabilizing the calculations. If both procedures are present, efficient stability is guaranteed over a larger range of parameters.

Something that needs an explanation is why the acceptance ratios of positive and negative walkers are significantly different in some cases: while this happens for both the SSIS functions used, it does not occur when SSIS is not included.

TABLE III: Fixed-node results obtained from our FMC method by setting $\psi_G = \psi_A$ and rejecting any move resulting in a change of the sign of ψ_A. The SSIS-denom and Acceptance/Rejection procedures have been used.

Time-step in K^{-1}	Length of the run (in τ_{rel})	E(ΔE) in K
1.2×10^{-4}	10	-2.3718(4)
6×10^{-5}	10	-2.369(2)
3×10^{-5}	3	-2.369(13)

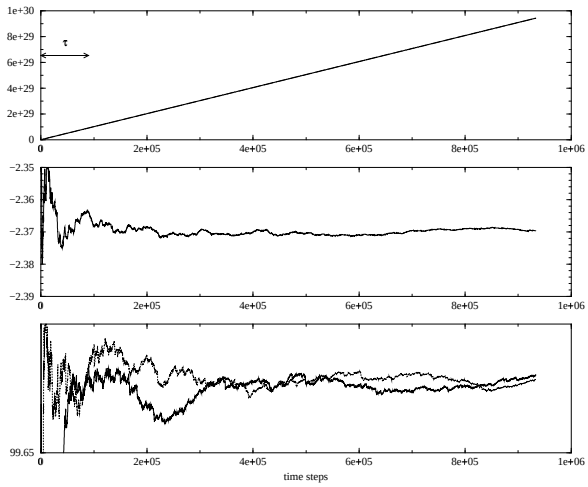

FIG. 8: Results for a fixed node limit -run. Top: cumulative denominator; Center: cumulative energy; Bottom: acceptance ratios (solid line: $\mathbf{R}^+$, dotted line: $\mathbf{R}^-$).

I. Population size effect and FXN limit

All the results shown here have been obtained with a population of 192 pairs, which has to be considered rather small. This gives rise to an important error in our estimations, resulting in higher energies. This is even more important in the case of FMC with respect to the FXN limit. Several fixed node results have been obtained using our correlated walkers scheme, by using the antisymmetric part only in the guiding wavefunction of formula (14) and rejecting all the walkers that cross the nodal surface.

Results are summarized in Table III and the behavior of quantities such as acceptance ratios, cumulative denominator and cumulative eigenvalue is shown in Fig. 8. These runs include SSIS in the denominator version.

Like the full, exact ones, these results have been obtained by using a set of 192 pairs of walkers. The FXN energy is lower than the FMC one. Nevertheless one should bear in mind that, although both the FMC and FXN suffer from some degree of population size effect, this effect depends on the quality of the guiding functions, which is a very good one for the FXN case (ψ_A alone), whereas the full ψ_G is not. Better comparison between FXN and FMC results would come from calculations done with a larger number of walkers, thus reducing the population size effect directly, or from calculations done with importance functions of better quality.

IV. ACKNOWLEDGMENTS

We gratefully thank David Ceperley, Geoffrey Chester, Berni Alder, Joseph Carlson, Kevin Schmidt, and Randolph Hood for stimulating comments. We are also indebted to David Hardin for a critical review of the manuscript. This work was performed under the auspices of the U.S. Department of Energy by the University of California, Lawrence Livermore National Laboratory under contract No. W-7405-Eng.-4, and funded by the Laboratory Directed Research and Development (LDRD) Program at Lawrence Livermore National Laboratory (LLNL) under project 01-LW-040.

* Electronic address: `colletti@science.unitn.it`
† Electronic address: `pederiva@science.unitn.it`
‡ Electronic address: `kalos1@llnl.gov`

[1] M. H. Kalos, D. Levesque, and L. Verlet, Phys. Rev. A **9**, 2178 (1974).
[2] D. M. Ceperley, Rev. Mod. Phys. **78**, 279 (1995).
[3] J. B. Anderson, J. Chem. Phys. **63**, 1499 (1975).
[4] J. B. Anderson, J. Chem. Phys. **65**, 4121 (1976).
[5] P. J. Reynolds, D. M. Ceperley, B. J. Alder, and J. W. A. Lester, J. Chem. Phys. **77**, 5593 (1982).
[6] D. M. Ceperley and B. J. Alder, Phys. Rev. Lett. **45**, 566 (1980).
[7] M. A. Lee, K. E. Schmidt, and M. H. Kalos, Phys. Rev. Lett. **46**, 728 (1981).
[8] M. H. Kalos, Phys. Rev. E **53**, 5420 (1996).
[9] Z. Liu, S. Zhang, and M. H. Kalos, Phys. Rev. E **50**, 3220 (1994).
[10] K. E. Schmidt, M. A. Lee, M. H. Kalos, and G. V. Chester, Phys. Rev. Lett. **47**, 807 (1995).
[11] D. M. Arnow, M. H. Kalos, M. A. Lee, and K. E. Schmidt, J. Chem. Phys. **77**, 5562 (1982).
[12] M. H. Kalos and K. E. Schmidt, J. Stat. Phys. **89**, 425 (1997).
[13] C. J. Umrigar, M. P. Nightingale, and K. J. Runge, J. Chem. Phys. **99**, 2865 (1993).
[14] T. R. Roberts, R. H. Sherman, and S. G. Sydoriak, Phys. Rev. **68**, 4 (1962).
[15] R. A. Aziz, V. P. S. Nain, J. S. Carley, W. L. Taylor, and G. T. McConville, J. Chem. Phys. **70**, 4330 (1979).
[16] T. R. Roberts, R. H. Sherman, and S. G. Sydoriak, J.Res.Nat.Bur.Stand.Sect.A **68**, 567 (1964).
[17] D. M. Ceperley, private communication.